Mutations in the Nucleotide-Binding Sites of P-Glycoprotein That Affect Substrate Specificity Modulate Substrate-Induced Adenosine Triphosphatase Activity†

Lucille Beaudet, Ina L. Urbatsch, and Philippe Gros*

Department of Biochemistry, McGill University, 3655 Drummond Street, Montréal, Québec, Canada H3G 1Y6

Received October 27, 1997; Revised Manuscript Received March 17, 1998

ABSTRACT: The amino- and carboxy-terminal nucleotide-binding domains (NBD1 and NBD2) of P-glycoprotein (P-gp) share over 80% sequence identity. Almost all of NBD1 can be exchanged by corresponding NBD2 segments with no significant loss of function, except for a small segment around the Walker B motif. Within this segment, we identified two sets of residues [ERGA → DKGT (522−525) and T578C] that, when replaced by their NBD2 counterparts, cause dramatic alterations of the substrate specificity of the protein [Beaudet, L., and Gros, P. (1995) *J. Biol. Chem. 270*, 17159−17170]. We wished to gain insight into the molecular basis of this defect. For this, we overexpressed the wild-type mouse Mdr3 and variants bearing single or double mutations at these positions in the yeast *Pichia pastoris*. P-gp-specific ATPase activity was measured in yeast plasma membrane preparations after detergent solubilization and reconstitution in *Escherichia coli* proteoliposomes. P-gp proteoliposomes from *P. pastoris* showed a strong verapamil- and valinomycin-stimulated ATPase activity, with characteristics (K_M, V_{max}) similar to those measured in mammalian cells. Mutations did not appear to affect the K_M for Mg^{2+}ATP (∼ 0.4 mM), but maximum velocity (V_{max}) of the drug-stimulated ATPase activity was severely affected in a substrate/modulator-specific fashion. Indeed, all mutants showed complete loss of verapamil-induced ATPase, while all retained at least some degree of valinomycin-induced ATPase activity. Photolabeling studies with [^{125}I]iodoarylazidoprazosin, including competition with MDR drugs and modulators, suggested that drug binding was not affected in the mutants. The altered drug resistance profiles of the ERGA → DKGT(522−525) and T578C mutants in vivo, together with the observed alterations in substrate-induced ATPase activity of these proteins, suggest that the residues involved may form part of a signal pathway between the membrane regions (substrate binding) and the ATP binding sites.

Multidrug resistance in cultured cells in vitro and in certain tumor cells in vivo is caused by the overexpression of P-glycoprotein (P-gp)[1] (reviewed in ref *1*). P-gps are encoded by a small family of three genes in rodents (*mdr1*, *mdr2*, and *mdr3*) and two genes in humans (*MDR1* and *MDR2*) (reviewed in ref *1*). P-gps are integral membrane proteins that bind photoactivatable analogues of drugs (*2*) and ATP (*3*), have ATPase activity (*4*−*7*), and function as direct drug efflux pumps (*8*) to reduce intracellular drug accumulation in resistant cells (reviewed in ref *1*). Physiological analyses of mutant mice bearing null alleles at *mdr* genes (*9*), as well as transport experiments in intact cells (*10*) or in isolated membrane vesicles expressing individual P-gps (*11*), have shown that the normal physiological role of the liver-specific Mdr2 P-gp (class II isoform) is a phosphatidylcholine (PC) flippase that translocates PC molecules from the inner to the outer leaflet of the bile canalicular membrane. Recent studies have suggested that the Mdr1 P-gp (class I isoform) may also function as a broad-specificity translocase for short-chain phospholipids (*12*). On the basis of these and other results, it has been proposed that P-gp may transport cytotoxic drugs by a translocase or flippase mechanism (*11*, *12*).

Sequence analyses suggest that P-gps are formed by two homologous halves, each encoding six putative transmembrane (TM) domains and one nucleotide-binding domain (NBD) (*13*). This structural unit is highly conserved in a large group of prokaryotic and eukaryotic proteins, known as the ABC family of membrane transporters (*14*). Topology predictions from hydropathy profiling (*13*), direct characterization by epitope tagging and immunofluorescence (*15*, *16*), and maleimide labeling in single cysteine mutants (*17*) have verified that P-gp contains 12 TM domains, with six in each half. A considerable body of data indicates that the TM domains play a key role in substrate binding. This includes (i) energy transfer experiments in intact cells

† This work was supported by research grants to P.G. from the Medical Research Council of Canada. P.G. is an International Research Scholar of the Howard Hughes Medical Institute and is a Career Scientist of the Medical Research Council of Canada.

* To whom all correspondence should be addressed: Phone 514-398-7291; FAX 514-398-7384; E-mail, gros@medcor.mcgill.ca.

[1] Abbreviations: ABC, ATP-binding cassette; *AOX1*, alcohol oxidase 1; CFTR, cystic fibrosis transmembrane conductance regulator; CHO, Chinese hamster ovary; DOC, deoxycholic acid, sodium salt; DTT, dithiothreitol; EACA, ϵ-amino-*n*-caproic acid; IAAP, [^{125}I]iodoarylazidoprazosin; MDR, multidrug resistance; MG, minimal glycerol; MM, minimal methanol; *mut*^{s}, methanol utilizing slow; NBD, nucleotide-binding domain; PC, phosphatidylcholine; P-gp, P-glycoprotein; PMSF, phenylmethanesulfonyl fluoride; SDS−PAGE, sodium dodecyl sulfate−polyacrylamide gel electrophoresis; TM, transmembrane domain; WT, wild type; YNB, yeast nitrogen base.

S0006-2960(97)02656-1 CCC: $15.00
Published on Web 06/02/1998

between a membrane photoactivatable probe, a fluorescent drug substrate, and P-gp (*18*); (ii) epitope mapping studies of proteolytic P-gp fragments labeled with photoactivatable drug analogues (*19*); and (iii) a large number of genetic studies showing that mutations within (*20*−*22*) or near (*23*, *24*) TM domains affect the substrate specificity of P-gp but also that of other ABC transporters such as TAP1/TAP2 (*25*) and CFTR (*26*).

The two NBDs of P-gp are located on the intracellular side of the membrane and are each defined by the presence of three sequence signatures: the consensus Walker A [G-$(X)_4$-G-K-S/T] and Walker B [R/K-$(X)_{6-8}$-L-$(Hyd)_4$-D] motifs (Hyd is hydrophobic) found in a number of ATP binding proteins and ATPases (*27*) and a short "linker peptide" of sequence L-S-G-G-$(X)_3$-R-Hyd-X-Hyd-A, which is located between the Walker A and B motifs and which is specific for ABC transporters. P-gp binds [^{32}P]-8-azido-ATP (*3*), and purified P-gp shows a robust ATPase activity [K_M for Mg^{2+}ATP of 1 mM, V_{max} of 0.3−2 μmol min^{-1} (mg of protein)$^{-1}$] (reviewed in ref *28*). A unique property of this ATPase activity is that it can be further stimulated by certain MDR drugs (e.g., vinblastine) or P-gp inhibitors (e.g., verapamil), while other drugs or modulators inhibit ATP hydrolysis (reviewed in refs *28* and *29*). These findings suggest that drug binding to TM domains transduces a signal to the NBD sites to hydrolyze ATP, and mediate transport, with inhibitors acting either as direct substrates or as uncouplers of this signal. Although the exact catalytic sequence of ATP hydrolysis by P-gp has not yet been fully characterized, mutagenesis studies have shown that both NBDs are essential for function (*30*), with ATP binding and hydrolysis occurring at both sites (*31*, *32*).

One of the key unresolved issue in the study of P-gp is the mechanism underlying signal transduction between TM domains and the NBDs, resulting in either activation of ATPase activity upon substrate binding to the TM domains, and/or substrate movement upon ATP hydrolysis at the NBDs. We have previously tested whether the two NBDs of P-gp are functionally equivalent and interchangeable and have investigated the segments and amino acids important for proper function of each NBD within the context of the C- or N-terminal P-gp half (*33*). For this, we constructed and tested the biological activity in yeast and mammalian cells of a series of chimeric *mdr3* cDNAs in which discrete domains of the N-terminal NBD (NBD1) were replaced by the homologous segments of the C-terminal NBD (NBD2) (*33*). We found that most NBD1 segments could be replaced by their NBD2 counterparts without loss of P-gp function, but exchange of a small segment near the Walker B motif caused a dramatic alteration in the drug resistance profile: while vinblastine resistance remained intact, adriamycin and colchicine resistance in CHO cells were impaired, as were FK506 resistance and *ste6* complementation in yeast. Site-directed mutagenesis at all divergent positions between NBD1 and NBD2 in this short segment indicated that amino acids at positions 522−525 (ERGA) and 578 (T) were responsible for the altered P-gp function, identifying these residues as essential for proper function of NBD1 in the context of the N-terminal half of P-gp (*33*). The ERGA → DKGT (522−525) mutant overlaps three amino acid substitutions immediately upstream from the LSGGQ signature of NBD1, while T578C maps in a conserved segment immediately downstream from the Walker B motif. The altered drug resistance phenotype observed in the ERGA → DKGT (522−525) and T578C NBD mutants is unusual and suggested that the residues involved may participate either directly or indirectly in substrate interactions or were implicated in signal transduction from NBDs to TM domains.

In the present study, we have used the methylotrophic yeast *Pichia pastoris* for the high-level expression of P-gp. We used a simple enrichment and reconstitution procedure to measure P-gp ATPase activity in *P. pastoris* membrane fractions. We have used this system to further characterize the biochemical basis of the altered substrate specificity of the NBD mutants at amino acid positions 522−525 (ERGA → DKGT) and 578 (T → C).

EXPERIMENTAL PROCEDURES

Plasmid Construction and Transformation. The expression system including *Pichia pastoris* yeast strain GS115 (*his4*) and expression vector pHIL-D2 were obtained from InVitrogen (license no. 145457). A 4.2 kb full-length mouse *mdr3* cDNA including 57 base pairs of 5′ and 210 base pairs of 3′ untranslated sequences was excised from vector pDR16 (*34*) using restriction enzymes *Kpn*I and *Cla*I (polylinker sites). The *Kpn*I/*Cla*I fragment was repaired with T4 DNA polymerase and inserted into the *Eco*RI site of plasmid pHIL-D2 similarly repaired with T4 DNA polymerase. The resulting plasmid, pHIL-*mdr3*, was propagated and purified from *Escherichia coli* according to standard protocols. Mutations ERGA → DKGT (522−525), T578C, and the combined ERGA → DKGT (522−525) and T578C mutant were introduced into pHIL-*mdr3* by direct replacement of an internal *mdr3* cDNA subfragment (from 1377 to 2249) by the corresponding mutated *mdr3* segments from pVT101-U constructs that we have previously described (*33*). pHIL-D2 expression constructs containing wild-type (WT) or mutant *mdr3* cDNAs were linearized with *Not*I and transformed into *P. pastoris* GS115 spheroplasts using a lithium acetate technique (*35*). *His*$^+$ transformants were streaked in parallel onto minimal methanol plates [MM: 1.34% (w/v) yeast nitrogen base (YNB), 0.04% (w/v) biotin, 0.5% (v/v) methanol, and 20% (w/v) agar] and on minimal glycerol plates [MG: 1.34% (w/v) YNB, 0.04% (w/v) biotin, 1% glycerol, and 20% (w/v) agar] to identify clones showing successful homologous recombination events at the *AOX1* locus. These clones manifest as impaired for growth on methanol as a sole carbon source (*m*ethanol *u*tilizing *s*low or *mut*^{s}). Several such *His*$^+$ *mut*^{s} transformants were isolated for each *mdr3* construct, expanded in culture, and stored frozen.

Membrane Preparation. Cell lysates and membrane fractions were prepared in ice-cold buffers supplemented with a cocktail of protease inhibitors consisting of leupeptine and pepstatin A (each at 10 μg/mL), ϵ-amino-*n*-caproic acid (EACA; 15 mM), *p*-aminobenzamidine (1 mM), and phenylmethanesulfonyl fluoride (PMSF; 1 mM). The initial screen for *P. pastoris* clones expressing P-gp was performed on crude cell lysates as follows: clones were inoculated in 5 mL of MG medium and grown overnight with strong agitation (250 rpm) at 30 °C up to an optical density (600 nm) of 1.5. Cells were recovered by centrifugation, resus-

pended in an identical volume of methanol-containing MM medium, and further incubated at 30 °C for 48 h to induce expression of the chromosomal *AOX1-mdr3* cassette. Crude lysates of methanol-induced cells were prepared by vigorous vortexing of the cells with acid-washed beads (8 × 30 s pulses at 4 °C) in 400 μL of a buffer containing 5% (v/v) glycerol, 50 mM sodium phosphate, pH 7.4, 1 mM EDTA, and protease inhibitors. Cell debris and glass beads were removed by centrifugation in a refrigerated microfuge (15000*g*, 10 min) and total cell lysates were recovered. Small-scale preparations of *P. pastoris* crude membranes were obtained from 100 mL cultures of induced cells according to a protocol we have previously described for *Saccharomyces cerevisiae* (*8*). Both total cell lysates and crude membrane extracts were used for initial detection of P-gp by SDS−PAGE (see below).

For large-scale preparations of *P. pastoris* membranes, 1−3 L cultures were grown in MG medium and induced in MM medium. Briefly, 500 mL cultures were induced in 2 L baffled flasks and methanol was replenished after 2 days. After a total of 3 days of methanol induction, cells were pelleted (1500*g*) and resuspended in $^1/_{20}$ volume of SM buffer (1.2 M sorbitol, 20 mM Tris-HCl, pH 7.0, and 5 mM EDTA) containing 20% glycerol and frozen at −80 °C. Crude membranes were prepared according to Perlin et al. (*36*) with small modifications: frozen cells were rapidly thawed out at 30 °C and concentrated by centrifugation to a density of 7.5 g/40 mL in ice-cold Buffer A [0.33 M sucrose, 150 mM Tris-HCl, pH 7.4, 1 mM EGTA, 1 mM EDTA, 1 mM dithiothreitol (DTT), and protease inhibitors]. Cells were passed twice through a French pressure cell (20 000 psi), with fresh PMSF added to the samples every 30 min. Large cell debris and unbroken cells were removed by centrifugation (14000*g*, 4 °C, 20 min) and crude membrane fractions were pelleted from the supernatant (200000*g*, 4 °C, 90 min). Crude membranes were resuspended and washed once in buffer B [10 mM Tris-HCl, pH 7.4, 1 mM EDTA, and 10% (v/v) glycerol], homogenized by three passages through a tight-fitting glass homogenizer, and concentrated by centrifugation (as above). The final crude membrane pellet was resuspended in 4 mL of ice-cold buffer B using a 23-gauge needle and layered on top of a discontinuous sucrose density gradient consisting of 16%, 31%, 43%, and 53% (w/v) sucrose solutions containing 10 mM Tris-HCl, pH 7.4, and 0.1 mM EDTA (TE), followed by centrifugation (53000*g*, 4 °C, 16 h). Membranes at the various interfaces of the gradient were collected, diluted to less than 0.25 M sucrose with TE, and recovered by centrifugation (200000*g*, 4 °C, 3 h). Membrane pellets were resuspended in buffer C (0.33 M sucrose, 40 mM Tris-HCl, pH 7.4, 1 mM EGTA, and 1 mM EDTA, 1 mM DTT) and stored frozen at −80 °C. Protein concentration of samples was determined by the bicinchoninic acid protein assay (*37*) with bovine serum albumin as reference standard.

SDS−PAGE Analysis and Immunoblotting. Proteins were separated on a 7.5% gel by sodium dodecyl sulfate−polyacrylamide gel electrophoresis (SDS−PAGE) according to Laemmli (*38*). After migration, gels were either stained with Coomassie brilliant blue R-250 or transferred to nitrocellulose. Immunodetection of P-gp was performed as previously described (*33*) using the anti-P-gp monoclonal antibody C219 (Signet Laboratories Inc.), and immune complexes were revealed with the ECL detection system (Amersham).

Photoaffinity Labeling with [^{125}I]Iodoarylazidoprazosin. For photolabeling of P-gp with drug analogues, crude membranes (2.5 mg/mL) were first equilibrated in TE by passage through a Sephadex G-50 spin column and then incubated in the dark for 30 min with the drug analogue [^{125}I]iodoarylazidoprazosin ([^{125}I]IAAP; 2200 Ci/mmol; New England Nuclear) at a final concentration of 30 nM, in the absence or in the presence of increasing excess of MDR drugs or P-gp modulators. Membranes were then irradiated with UV for 1 min on ice, as previously described (*39*). Free [^{125}I]IAAP was removed by centrifugation (150000*g*, 4 °C, 30 min) in a tabletop ultracentrifuge (Beckman; rotor TL-100). Membrane pellets were dissolved in sample buffer for 30 min at 23 °C and separated by SDS−PAGE (7.5% gel). Gels were dried and exposed overnight at −80 °C to Kodak X-AR films with one intensifying screen or were exposed for 4 h to a phospho-imaging plate (type BASIII, Fuji) and the signal intensity was quantitated using a Bio-Image Analyzer (Fuji).

P-gp Solubilization and Reconstitution in E. coli Lipids. P-gp was solubilized from the membrane fraction recovered at the interface of the 16% and 31% (w/v) sucrose gradient interface (16/31 membranes) using deoxycholic acid sodium salt (DOC) by a modification of published protocols (*40*, *49*). Briefly, 16/31 membranes were solubilized at a final concentration of 1 mg/mL in buffer D [0.33 M sucrose, 40 mM Tris-HCl, pH 7.4, 1 mM EGTA, 1 mM EDTA, 1 mM DTT, 1.4% (w/v) DOC, 20% (v/v) glycerol, and 0.4% (w/v) *E. coli* lipids] by gentle vortexing at 20 °C. Once solubilized, samples were ice-cooled and spun at 200000 g for 1 h at 4 °C to remove insoluble material. *E. coli* lipids, dissolved in buffer C, were then added to the solubilized fraction to a final concentration of 1.4% (w/v). Reconstitution was achieved by dialysis against 200 volumes of 40 mM Tris-HCl, pH 7.4, 0.1 mM EGTA, 1 mM DTT, and 5 mM EACA at 4 °C for 48 h. Reconstituted samples were aliquoted and stored at −80 °C. The percentage of P-gp (w/w) present in the reconstituted samples was evaluated by laser densitometry of the samples separated on an SDS−10% polyacrylamide gel and stained with Coomassie blue using the Sci-Scan 500 densitometer (U.S. Biochemical Corp.).

ATPase Activity. ATPase activity of the reconstituted fractions was estimated by measuring inorganic phosphate release by the colorimetric phosphate determination method of Van Veldhoven and Mannaerts (*41*). Basic ATPase cocktail consisted of 40 mM Tris-HCl, pH 7.4, 10 mM ATP, and 10 mM $MgCl_2$. EGTA (0.1 mM) and sodium azide (10 mM) were included to eliminate possible contamination by Ca^{2+} ATPase and from F_1 ATPase, respectively. One to three micrograms of protein was added to 50 μL of cocktail and incubated for 10−40 min at 37 °C. Both protein concentration and time of incubation were kept within the linear range of the ATPase reaction. For measurements of pH dependence of ATPase activity, the pH of the cocktails was adjusted at 37 °C with 50 mM Tris-succinate (pH 4.7−8.5). P-gp substrates or modulators were added from fresh stocks in dimethyl sulfoxide.

Transport Assay. Drug-sensitive control CHO cells and transfected cell clones expressing wild-type or mutant Mdr3

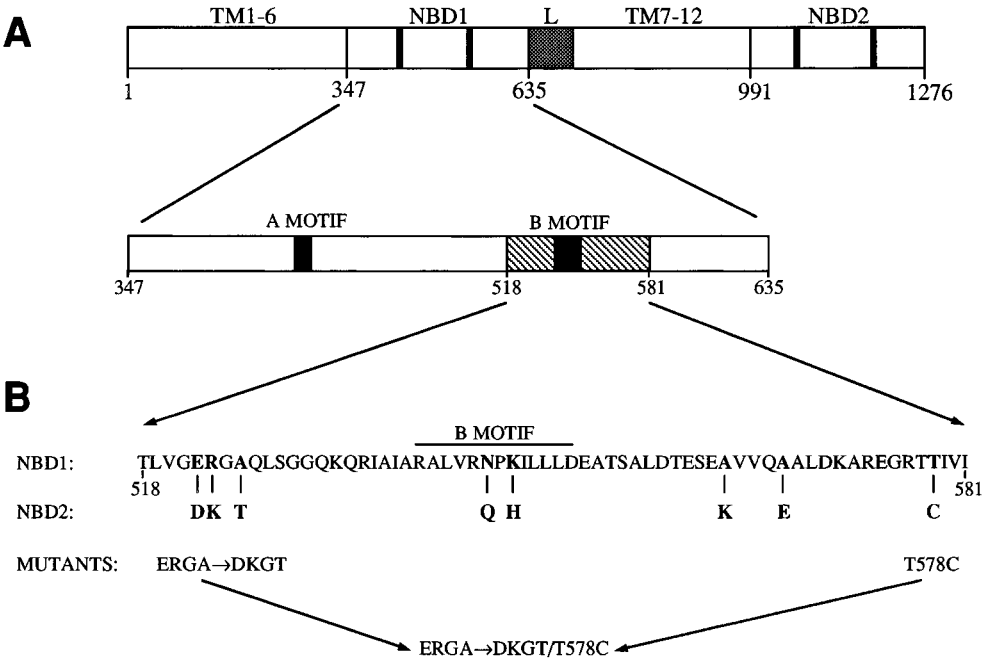

FIGURE 1: Schematic representation of structural domains of Mdr3 and localization of NBD1 mutants. (A) Structural domains in the Mdr3 protein include transmembrane segments (TM1−6 and TM7−12), nucleotide binding domains (NBD1 and NBD2), and linker region (L). Enlarged section represents the entire NBD1 from the end of TM6 to the beginning of the linker region. Positions of the Walker A and B motifs are marked by black boxes. The chimeric construct in which replacement of NBD1 by the corresponding NBD2 segment caused altered drug resistance in mammalian cells (*33*) is shown as a hatched box. (B) Identification of nonconserved residues between NBD1 and NBD2 and positions of individual and double mutants previously created by site-directed mutagenesis (*33*).

variants were grown to confluency and harvested after trypsin treatment (2 min at 37 °C). Cells were washed once with PBS and allowed to recover for 2 h at room temperature in complete culture medium (*30*). The cell suspensions were adjusted to 8×10^6 cells/mL in PBS containing 10 mM glutamine and 10 mM glucose at 20 °C, and transport was initiated by adding [^{3}H]vinblastine (specific activity 15.5 Ci/mmol; Amersham) to a final concentration of 100 nM (*30*). At given times, 0.5 mL aliquots were centrifuged (10 s at 10000*g*) through a 4:1 mixture of silicon oil and mineral oil, the supernatants and oil were removed, and the cell pellets were dissolved overnight in 1 N NaOH. The digests were neutralized by the addition of an equal volume of 1 N HCl, 100 μL aliquots were spotted on filter disks and dried, and the incorporated radioactivity was measured by liquid scintillation spectrometry. Total cell protein in the digests was measured with an amido black-based commercial assay (Bio-Rad), and results were expressed as counts per microgram of protein.

Drugs and Chemicals. Cytotoxic drugs and reagent-grade chemicals were purchased from Sigma. Verapamil was obtained from ICN; valinomycin was from Calbiochem. Acetone/ether-precipitated *E. coli* lipids were purchased from Avanti Polar Lipids and 2-deoxycholic acid sodium salt was from American Chemicals Ltd.

RESULTS

Expression of Mdr3 in the Yeast Pichia pastoris. We have previously identified two sets of residues [amino acid positions 522−525 (ERGA) and 578 (T)] near the Walker B motif of NBD1 of P-gp (Figure 1) that cannot be substituted by their counterpart in NBD2 without loss of function (*33*). Interestingly, loss of function is expressed at the level of substrate specificity, as both the ERGA → DKGT (522−525) and T578C mutants retain the ability to confer resistance to vinblastine but can no longer confer resistance to other MDR drugs such as colchicine, adriamycin, and actinomycin D in CHO cells (Table 1). The capacity of these mutants to convey cellular resistance to vinblastine is paralleled by a concomitant ability of ERGA → DKGT (522−525), T578C, and the double ERGA → DKGT/T578C mutants to restrict intracellular accumulation of [^{3}H]vinblastine in these cells (Figure 2). Likewise, these mutants cannot convey resistance to the antifungal drug FK506, nor can they complement *ste6* in yeast (*33*), but they still retain the ability to confer cellular resistance to valinomycin (Table 1). The molecular basis for the unique phenotype of these mutants was investigated. For this, we expressed WT Mdr3 as well as the mutants ERGA → DKGT (522−525), T578C, and the double mutant (referred to as T578C + ERGA/DKGT) in the membrane of the methylotrophic yeast *Pichia pastoris*.

Table 1: Drug Resistance of Wild-Type and Mutant Mdr3 Variants in CHO Cells and *S. cerevisiae* Cells

	CHO[a]				*S. cerevisiae*[b]	
Mdr3	VBL	COL	ADM	ACT	FK506	Val
WT	+++	+++	+++	+++	+++	+++
ERGA/DKGT	+++	+	+	+	++	++
T578C	+++	+	+	+	++	+++
ERGA/DKGT+T578C	+++	±	±	±	+	+

[a] Drug cytotoxicity in CHO cells was measured by a sulforhodamine B assay (*33*). [b] Drug cytotoxicity in the yeast *S. cerevisiae* was determined by a growth inhibition assay in liquid medium in the presence of 50 μg/mL FK506 (*33*) or 25 μg/mL valinomycin: WT, 100%; ERGA/DKGT, 65%; T578C, 100%; ERGA/DKGT + T578C, 22%. ADM, Adriamycin; ACT, actinomycin D; COL, colchicine; Val, valinomycin.

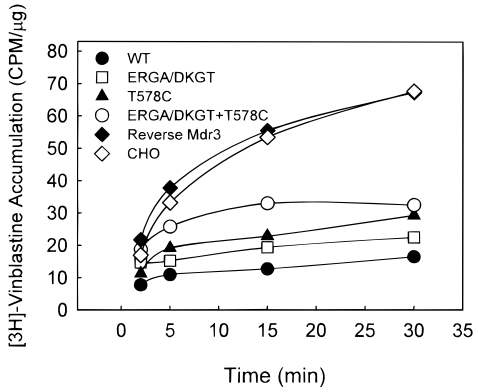

FIGURE 2: Vinblastine accumulation in cells expressing either wild-type or mutant Mdr3 variants. Drug-sensitive control CHO cells (◇) or cells transfected with the expression vector with the *mdr3* cDNA in the reverse orientation (◆), as well as cells expressing wild-type Mdr3 (WT, ●) or the ERGA/DKGT (□), T578C (▲), and ERGA/DKGT + T578C mutants (○) were incubated with [^{3}H]vinblastine (15.5 Ci/mmol; final concentration 100 nM). At predetermined times, cell-associated radioactivity was determined and presented as counts per minute per microgram of cellular protein. Each measurement was done in duplicate.

Full-length WT and mutant *mdr3* cDNAs were subcloned into the cloning polylinker of *P. pastoris* expression plasmid pHIL-D2. In this plasmid, the cloning site is flanked on either side by sequences corresponding to the *AOX1* 5′ and 3′ gene regions. Upon homologous recombination at the chromosomal *AOX1* locus, WT and mutant *mdr3* cDNAs are placed under the control of the strong methanol-inducible *AOX1* promoter. Addition of methanol to the medium arrests the growth of pHIL-D2 transformants showing homologous recombination (lack of functional copy of the *AOX1* gene) but induces high-level expression of *mdr3* RNA and proteins in these cells. *mdr3* pHIL-D2 constructs were transformed into GS115 *P. pastoris* spheroplasts, *His*$^+$ transformants unable to grow on methanol-containing medium (between 10% and 20% of *His*$^+$ transformants) were expanded in culture, and P-gp-expressing clones were identified by immunoblotting on crude cell lysates with the anti-P-gp antibody C219 (data not shown). Among *mut*^{s} clones analyzed, P-gp expression was detected in 70% of them and two such clones for each WT and mutant construct were used to prepare crude membrane extracts. These membrane proteins were separated by electrophoresis on a 7.5% polyacrylamide gel followed by direct staining with Coomassie blue (Figure 3A). We detected an abundant 140 kDa species in membrane fractions from all *mdr3* transformants analyzed, which was absent in membranes from control *P. pastoris* cells transformed with the pHIL-D2 vector alone. Immunoblotting of this gel with the anti-P-gp monoclonal antibody C-219 (Figure 3B) confirmed that the abundant 140 kDa species present in *mdr3* transformants was indeed Mdr3. These results indicate that WT and mutant Mdr3 variants can be stably expressed in the membrane fraction of the yeast *P. pastoris*.

Photoaffinity Labeling of WT and Mutant Mdr3 Variants with [^{125}I]Iodoarylazidoprazosin. The effect of the catalytic site mutations ERGA/DKGT and T578C and the T578C + ERGA/DKGT double mutation on the ability of Mdr3 to bind a radiolabeled drug analogue was studied by using [^{125}I]-iodoarylazidoprazosin (IAAP), which shares a common binding site on P-gp with several other P-gp substrates,

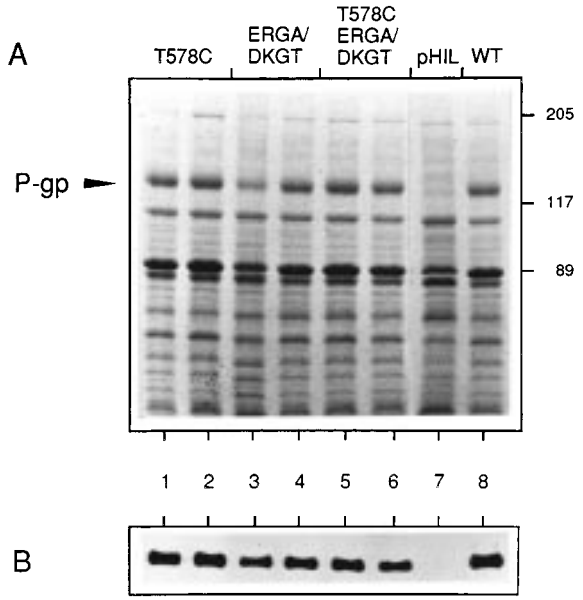

FIGURE 3: Detection of Mdr3 and mutant variants in crude membrane extracts from *P. pastoris*. (A) Crude membrane extracts were prepared from two individual clones of each mutant *mdr3* transformant (lanes 1−6), a negative control transformed with the pHIL-D2 vector (pHIL, lane 7), and a positive control transformed with wild-type *mdr3* (lane 8). Fifteen micrograms of protein were loaded in each lane, separated by SDS−PAGE, and stained with Coomassie blue. (B) Western blot analysis of the samples shown in panel A with the anti-P-gp monoclonal antibody C219.

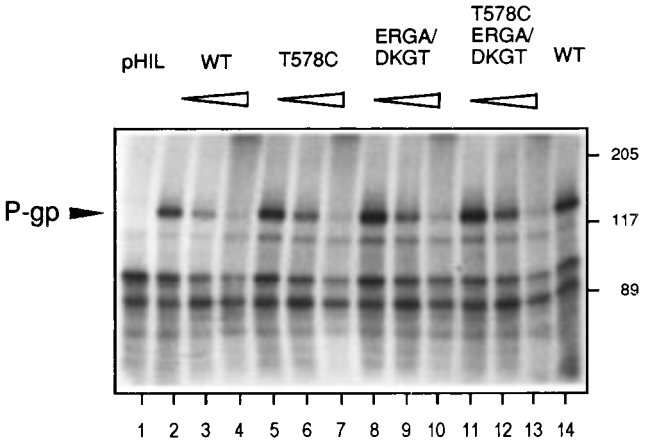

FIGURE 4: Photolabeling of wild-type and mutant Mdr3 variants by IAAP. Photolabeling in the absence (lanes 2, 5, 8, 11, and 14) or presence of 150 μM (lanes 3, 6, 9, and 12) and 3 mM (lanes 4, 7, 10, and 13) vinblastine. The position of the 140 kDa P-gp after SDS−PAGE and autoradiography is indicated by an arrowhead. Photolabeling of the 140 kDa species was completely absent in membranes from a control pHIL clone (lane 1). Molecular mass markers are indicated at the right-hand side of the gel. Similar results were obtained in two independent experiments.

including vinblastine (*42*). *P. pastoris* membranes expressing WT or mutant Mdr3 variants were incubated with IAAP in the absence or presence of increasing concentrations of several MDR drugs (vinblastine, valinomycin, FK506) or P-gp modulators (verapamil), followed by cross-linking with UV (data are shown for vinblastine in Figure 4). Non-incorporated IAAP was removed by centrifugation and photolabeled species were directly analyzed by SDS−PAGE and autoradiography (Figure 4). We have previously shown that wild-type (WT) Mdr3 is readily labeled by IAAP as a 140 kDa species that is absent from membranes of control

cells transformed with the pHIL-D2 vector (Figure 4, pHIL) (*62*). Photolabeling of the 140 kDa Mdr3 species by IAAP is competed by increasing concentrations of the P-gp substrate vinblastine (Figure 4) and valinomycin, while colchicine and doxorubicin have little effect on IAAP labeling of the wild-type Mdr3 (*62*). Similar results were obtained with the ERGA/DKGT, T578C, and T578C + ERGA/DKGT mutants (Figure 4). Quantitation of the radioactive signal of the 140 kDa Mdr3 band in each sample for Figure 4 (data not shown) confirmed similar competitive interactions between IAAP and vinblastine for the WT and mutant Mdr3 variants. Indeed, vinblastine reduced binding of IAAP to wild type and to the ERGA/DKGT, T578C, and T578C + ERGA/DKGT mutants by 60% ± 5% (150 μM) and by 80% ± 6% (3 mM). Valinomycin (150 μM) reduced IAAP labeling of wild-type and mutant Mdr3 variants by 57% ± 7% in all cases. FK506 was found to be a poor competitor in all cases (30% ± 10%, at 90 μM), while verapamil did not affect IAAP photolabeling even at the highest concentration tested (300 μM). These results indicate that (1) Mdr3 expressed in *P. pastoris* is correctly folded and binds IAAP with characteristics similar to those detected in mammalian cells membranes and (2) the three mutant variants can bind IAAP with characteristics similar to Mdr3 and are also correctly folded in *P. pastoris* membranes. Together, these results indicate that the ERGA/DKGT, T578C, and T578C + ERGA/DKGT mutations do not have major effects on the drug binding properties of P-gp.

ATPase Activity of Mdr3 Expressed in P. pastoris. As a first step in analyzing the effect of the three mutations on the ATPase activity of Mdr3, we monitored the presence of a possible drug-stimulatable ATPase activity in crude membrane preparations from *P. pastoris* expressing WT Mdr3. In such preparations, we detected strong ATPase activity that was identical in control and Mdr3-expressing membranes and that could not be stimulated by P-gp substrates or modulators such as verapamil (*62*). Analysis of the pH dependence of this ATPase activity indicated an optimal pH around 6.0 (data not shown), which is distinct from the reported optimal pH for P-gp ATPase (pH 7.6) but reminiscent of that of the endogenous yeast plasma membrane PMA-1 H^+-ATPase (reviewed in ref *43*). Consequently, we used an enrichment protocol aimed at purifying P-gp away from endogenous contaminating ATPases. Briefly, this protocol consisted of three basic steps: (1) sucrose gradient separation of the *P. pastoris* membrane fractions and isolation of the plasma membranes sedimenting at the 16%/31% interface; (2) differential deoxycholate (DOC) extraction of P-gp from these membranes, and finally (3) dialysis and reconstitution in *E. coli* proteoliposomes (Experimental Procedures). SDS−PAGE analysis of this detergent-extracted and reconstituted fraction from Mdr3-expressing membranes (Figure 5, WT) clearly shows the presence of P-gp with characteristics of electrophoretic mobility similar to that seen in the crude membrane extracts (Figure 3). From 1 L of *P. pastoris* culture, we routinely obtained around 10 mg of 16/31 membrane protein, 70% of which is extracted by DOC and reconstituted in *E. coli* lipids. In such reconstituted fractions, we were able to detect robust verapamil-induced, Mdr3-associated ATPase activity (Figure 6A). The optimum pH for this activity is around 7.8 (Figure 6A), consistent with published optimal pH values for P-gp

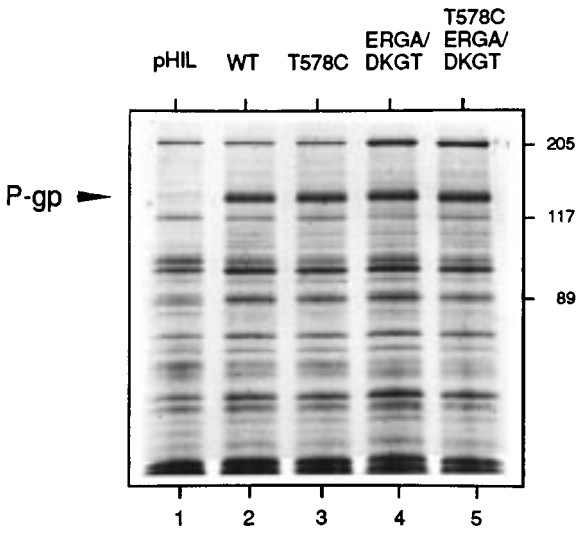

FIGURE 5: Coomassie-stained SDS−polyacrylamide gel of wild-type Mdr3 and mutant variants reconstituted in proteoliposomes. Crude membranes from *P. pastoris* clones transformed with either pHIL-D2 (pHIL), wild-type *mdr3* (WT), or the various *mdr3* mutants were fractionated on sucrose gradients and plasma membranes sedimenting at the 16%/31% interface were solubilized in deoxycholate and reconstituted in *E. coli* lipids (see Experimental Procedures). Fifteen micrograms of protein was run in each lane.

expressed in mammalian and other membranes (reviewed in ref *28* and *29*). Under conditions of optimum verapamil stimulation (100 μM), this ATPase activity peaks at 0.160 μmol mg^{-1} min^{-1}, which corresponds to a 4.4-fold stimulation above background levels monitored in the absence of verapamil (Figure 6B), also consistent with published reports on P-gp expressed in other systems (*28, 29, 50, 54*). This ATPase activity can also be stimulated about 6-fold by valinomycin (optimum 100 μM; Figure 6C) but only 2.6-fold by vinblastine (30 μM; Figure 6D).

ATPase Activity of NBD1 Mutants. The same protocol was used to monitor the effect of the NBD1 mutations on ATPase activity. Reconstituted proteoliposome preparations from WT and mutant P-gp-expressing *P. pastoris* transformants were separated onto 7.5% polyacrylamide gels followed by staining with Coomassie-blue (Figure 5). This analysis showed similar amounts of P-gp in all samples tested, and estimates obtained by laser densitometry indicated that P-gp accounted for 6−7% (w/w) of the reconstituted proteins in all samples. To monitor the effect of the ERGA/DKGT, T578C and T578C, + ERGA/DKGT mutations on P-gp ATPase activity, drug-inducible ATPase activity was investigated in these reconstituted detergent fractions (Figure 6). The modulatory effect of drugs to which cellular resistance in CHO cells is affected by the mutations was first investigated. Unfortunately, colchicine, adriamycin, and actinomycin D had no measurable stimulatory effect on the ATPase activity of wild-type and mutant Mdr3 variants in our experimental system even at the highest concentration tested (data not shown). Vinblastine was found to be a poor stimulator of wild-type P-gp ATPase in our system (2.6-fold), and no stimulation was detected in any of the mutants tested (Figure 6D). On the other hand, the best stimulator of ATPase activity in our experimental system was valinomycin, which gave an optimum 6-fold induction of Mdr3 ATPase activity at 100 μM (Figure 6C) with a specific activity of 0.209 μmol mg^{-1} min^{-1}. The specific activity

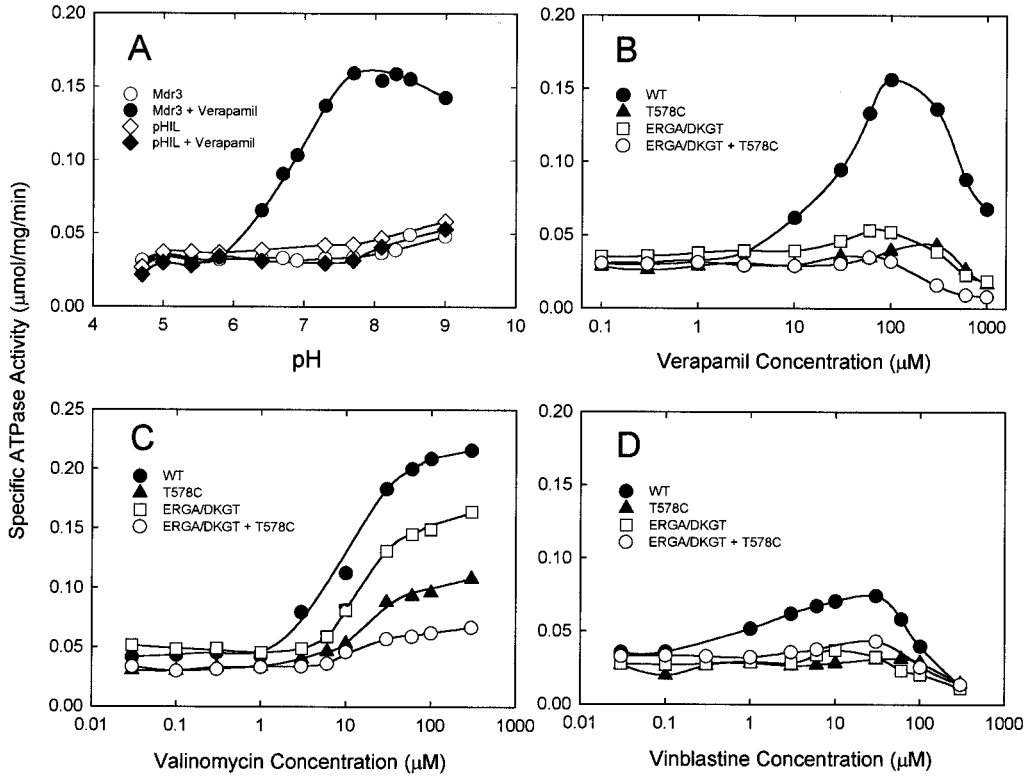

FIGURE 6: Stimulation of the ATPase activity of wild-type Mdr3 and mutant Mdr3 variants. Reconstituted proteoliposomes from *P. pastoris* clones transformed with control pHIL-D2 plasmid or expressing wild-ype or mutant Mdr3 variants were prepared as outlined in Experimental Procedures. (A) ATPase activity of reconstituted proteoliposomes from control pHIL-D2 (pHIL; ◇, ◆) or wild-type Mdr3 (WT; ○, ●) was measured as a function of pH in the absence (open symbols) or presence (solid symbols) of verapamil (100 μM). ATPase activity of wild type (WT, ●) and mutant Mdr3 variants ERGA/DKGT (□), T578C (▲), and ERGA/DKGT + T578C mutants (○) in the presence of increasing concentrations of verapamil (B), valinomycin (C), and vinblastine (D). Similar results were obtained in two independent experiments.

of the valinomycin-stimulated ATPase was reduced to 0.150 μmol mg^{-1} min^{-1} in the case of the ERGA/DKGT mutant (3.9-fold stimulation), to 0.096 μmol mg^{-1} min^{-1} for the T578C mutant (2.6-fold) and to 0.062 μmol mg^{-1} min^{-1} in the double mutant ERGA/DKGT-T578C (1.5-fold), a value barely above background levels measured either in the absence of drugs or in control membranes lacking P-gp (0.04 μmol mg^{-1} min^{-1}). When verapamil was used to monitor drug-induced ATPase activity, we observed a 4-fold stimulation for WT Mdr3 at 100 μM verapamil (specific ATPase activity of 0.152 μmol mg^{-1} min^{-1}) (Figure 6B), but a complete loss of verapamil-inducible ATPase activity was noted in proteoliposomes from either of the three ERGA/DKGT, T578C, and T578C + ERGA/DKGT mutants (Figure 6B). These results suggest that the three mutations in NBD1 analyzed here impair either partly or totally the drug-stimulatable ATPase activity of Mdr3, depending on the modulator used in the analysis.

To determine if the loss of drug-stimulatable ATPase activity in the mutants was associated with a decreased affinity of the protein for Mg^{2+}ATP as opposed to a loss in catalytic activity, the specific activity of WT and mutant variants of Mdr3 was measured at increasing concentrations of Mg^{2+}ATP (velocity plot) under conditions of optimal drug stimulation (100 μM valinomycin) and results are shown in Figure 7. The V_{max} and K_M for Mg^{2+}ATP for the WT and mutant Mdr3 variants were calculated and are presented in Table 2. The maximal velocity for the WT Mdr3 isoform in the presence of valinomycin was 0.210 μmol mg^{-1} min^{-1}, which can be extrapolated to a specific activity of 3.4 μmol

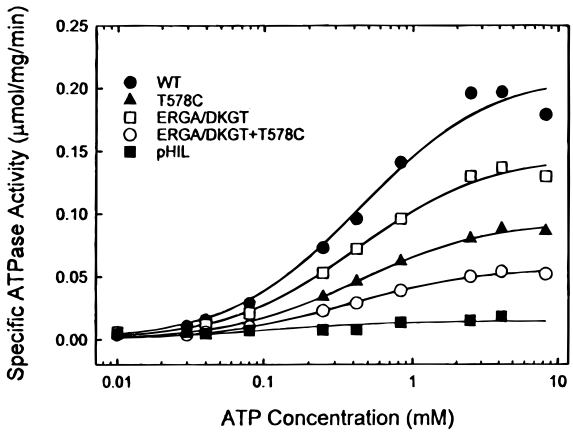

FIGURE 7: Mg^{2+}ATP dependence of ATP hydrolysis in *P. pastoris* membranes expressing wild-type Mdr3 or mutant Mdr3 variants. ATPase activity of reconstituted proteoliposomes expressing wild-type Mdr3 and mutant Mdr3 variants was measured in the presence of 100 μM valinomycin as a function of Mg^{2+}ATP concentration as described under "Experimental Procedures" except that an excess 2 mM Mg^{2+} was added to the assay medium. Curves are fits of the data to the Michaelis−Menten equation by nonlinear least-squares regression analysis.

mg^{-1} min^{-1} for a pure P-gp preparation. V_{max} values are decreased for the three Mdr3 variants (Table 2) in agreement with the specific activity values measured under similar stimulation conditions in Figure 6. In the mutants, reductions in V_{max} values were clearly not associated with a decrease in affinity for Mg^{2+}ATP, with WT and mutant Mdr3 variants showing very similar K_M values, around 0.4 mM (Table 2).

Table 2: Characteristics of the ATPase Activity of Wild-Type and Mutant Mdr3 Variants

clone	V_{max}[a]	K_M[b]
WT Mdr3	0.210	0.44
ERGA/DKGT	0.145	0.43
T578C	0.094	0.43
ERGA/DKGT-T578C	0.056	0.37
pHIL	0.040	ND

[a] V_{max} in micromoles per minute per milligram in the presence of 100 μM valinomycin (to achieve maximal stimulation). [b] K_M in millimolar as determined from Figure 7.

DISCUSSION

The mechanism by which P-gp transports drugs in general, and the mechanism by which binding of substrates or modulators to the TM domains stimulates ATP hydrolysis, remain poorly understood. To identify protein segments and residues in the nucleotide binding domains (NBD) possibly involved in this process, we created and studied chimeric molecules in which small segments of the C-terminal ATP binding site (NBD2) were substituted into the corresponding portions of NBD1. We observed that the replacement of NBD1 segments near the Walker B motif by the corresponding NBD2 segments resulted in a dramatic loss of function, and we were able to narrow down the deleterious effect to two series of residues, ERGA to DKGT replacement at positions 522−525 as well as the T578C substitution (*33*). The loss of function in these mutants was expressed as a dramatic change in substrate specificity (Table 1) (*33*). Such alterations in substrate specificity have been previously reported for mutations in the TM domains (*21*, *22*, *44*) but are very unusual for mutants in the NBD sites (*45*). Indeed, mutations in the NBDs more generally affect the overall transport function and such mutants (Walker A motif) are inactive in cellular drug resistance and drug transport studies and in all cases tested show a complete loss of ATPase activity (*30*, *46*, *47*).

An expression system in the yeast *Pichia pastoris* was selected for the overexpression of P-gp (Mdr3). We showed previously that P-gp can be functionally expressed in the yeast *S. cerevisiae*, as a nonglycosylated 140 kDa protein that (1) conveys cellular resistance to anticancer and antifungal drugs (*33*, *39*), (2) carries out vectorial drug transport in inside-out vesicles (*48*) or in secretory vesicles (*8*), and (3) has phosphatidylcholine translocase activity (*11*) and complements a mutation at the endogenous *STE6* locus (*39*). In the present study, P-gp could be expressed in *P. pastoris* as a stable, unglycosylated, and very abundant polypeptide of 140 kDa,accounting for approximately 7% of the membrane proteins. This P-gp appears to be folded properly in *P. pastoris* membranes, as it binds the photoactivatable IAAP with characteristics (competitive interactions) similar to that of P-gp expressed in membranes of *S. cerevisiae* (*39*) or of mammalian cells (*3*). In addition, this P-gp preparation showed stimulated ATPase activity (V_{max} up to 0.21 μmol min^{-1} mg^{-1}, K_M of 0.4 mM) upon incubation with various MDR drugs or P-gp modulators, including verapamil, valinomycin, gramicidin D, tetraphenylphosphonium, diethylstilbestrol, and FK506 (Figure 6 and data not shown). These noted characteristics are very similar to those reported for P-gp expressed in mammalian (*5*−*7*, *49*, *50*) or insect cells (*51*). A potential limitation of this system was the presence in various membrane fractions of contaminating H^+/ATPase PMA-1 (optimum pH 6.0); however, the inclusion of a DOC extraction step followed by reconstitution in *E. coli* lipids was sufficient to eliminate the contaminating activity (Figure 6A). Therefore, *P. pastoris* provides a very inexpensive, rapid, and reliable system to express very high amounts of biologically active P-gp.

The ERGA/DKGT, T578C, and ERGA/DKGT + T578C variants were expressed in *P. pastoris* for functional analysis. We considered the possibilities that the mutations affected (1) protein interaction with substrates at or near the binding site or (2) a substrate-induced catalytic activity of the protein. The first possibility was addressed by monitoring the effect of the mutations on the ability of the protein to react with the photolabeled drug analogue iodoarylazidoprazosin (IAAP). This molecule has been previously shown to bind P-gp (*42*, *52*) at a binding site common to several of the P-gp substrates (*42*) and has been used to monitor the effect of mutations on drug binding by P-gp (*39*, *53*). The three mutations analyzed (ERGA/DKGT, T578C, and ERGA/DKGT + T578C) did not appear to affect the IAAP binding characteristics, which were similar to WT Mdr3, with respect to binding the probe and competitive interaction with vinblastine (Figure 4), valinomycin, and FK506. The second possibility was tested by monitoring the effect of the mutations on ATPase activity. We observed that valinomycin and verapamil strongly stimulated the ATPase activity of the wild-type Mdr3 in our assay system, and we used these two drugs together with vinblastine (Figure 6). Other drugs, such as adriamycin, colchicine, and actinomycin D are poor stimulators, which renders difficult a parallel analysis of profiles of drug resistance and drug-stimulated ATPase caused by our mutants. A strong deleterious effect of the mutations on drug-stimulatable ATPase activity was noted for all three mutations. In addition, the extent of modulation of ATPase activity was dependent on the stimulator used: in the case of the ERGA/DKGT and T578C single mutants, readily detectable levels of ATPase activity were induced by valinomycin (Table 2), while both mutants were unresponsive to verapamil in the same assay (activity near background at 0.04 μmol min^{-1} mg^{-1}). On the other hand, the ERGA/DKGT + T578C double mutant showed only a weak amount of valinomycin-stimulated ATPase above background (Figure 6C) but was also nonresponsive to verapamil stimulation (Figure 6B).These differences in activity between the mutants were linked neither to different amounts of mutant proteins present in the reconstituted detergent fractions and introduced in the assay (Figure 5) nor to the relative affinity of the mutant NBDs for Mg^{2+}ATP, as all mutants showed K_M values for Mg^{2+}ATP in the range of that measured for WT Mdr3 (Table 2). Therefore, these experiments suggest that the molecular basis for the altered substrate specificity noted in the ERGA/DKGT, T578C, and ERGA/DKGT + T578C mutants was not through impaired drug binding but rather through selective impairment of the normal profile of substrate- or modulator-induced ATPase activity.

It is interesting to note that the three P-gp mutants tested, in particular the ERGA/DKGT + T578C double mutant with only 10−20% of WT levels of valinomycin-induced ATPase activity, can still convey resistance to vinblastine very efficiently in CHO cells (*33*) (Table 1). As shown in Figure

2, all mutants were able to reduce the intracellular accumulation of [^{3}H]vinblastine, suggesting that they are competent for drug transport. Unfortunately, the low stimulatory effect of vinblastine on ATPase activity of WT Mdr3 in our system (2.6-fold) precluded an accurate evaluation of the modulatory effect of this drug on the ATPase activity of our mutants, including the extent of possible loss of this activity.

How do these results fit current mechanistic models of P-gp action? The structural and functional importance of the membrane-associated regions and the NBDs in substrate binding and ATPase activity, respectively, has been convincingly established by biochemical and genetic approaches (reviewed in ref *1*). The mechanisms involved in signal transduction between these two regions are much more speculative. Indeed, while certain compounds such as verapamil and vinblastine stimulate ATPase, others like cyclosporin A do not stimulate the ATPase activity but can nevertheless inhibit stimulation by verapamil (*29*). In addition, other compounds completely inhibit P-gp ATPase activity (reviewed in ref *29*). These observations have led to the concept that substrate binding to the TM domains of P-gp stimulates ATP hydrolysis by the NBDs. While certain modulators that are transported by P-gp would mimic substrates and stimulate ATPase activity, others that are not transported would simply bind to TM domains and would uncouple the stimulatory signal to the NBDs (*28*, *29*). The phenotypic characteristics of the mutants studied in this report, which include altered substrate specificity in vivo and altered drug-induced ATPase activity, are consistent with the hypothesis that these residues participate in such a signal transduction pathway. It is interesting to note that the altered drug resistance profile of the G185V mutation in the human MDR1 (*23*, *55*) has also been found associated with alterations in the pattern of drug-stimulatable ATPase activity (*56*, *57*). This mutation maps in the first intracellular loop of P-gp and has been shown to cause increased resistance to colchicine and reduced resistance to vinblastine (*23*, *55*). ATPase measurements in insect cells expressing either the G185 or V185 MDR1 isoforms have detected similar levels of vinblastine-induced ATPase activity but striking differences in colchicine-induced (*57*) ATPase activity. Another NBD mutation known to affect substrate specificity is the enhanced colchicine resistance noted in the K536R variant of human MDR1 (*45*). Remarkably, K536R maps within the highly conserved dodecapeptide segment immediately upstream from the Walker B motif and immediately downstream from the ERGA/DKGT substitution studied in this report. The biochemical basis of the altered drug resistance profile in the K536R mutation has not yet been clarified, although it did not seem to affect binding of the photoactive probe [^{125}I]iodomycin (*45*). Together, these data suggest that K536, ERGA(522−525), T578, and perhaps G185 all participate in signal transduction events between membrane-associated regions and NBDs of the protein either to transmit a signal to NBDs upon drug binding to the TM regions or to transmit of a signal to TM domains upon ATP hydrolysis to mediate efflux, or both.

Although highly speculative, such a model is supported by additional observations made in an unrelated ABC transporter. A residue mapping to the homologous position of the T578C mutation studied here has been found to play a critical role in the maltose transport system of *E. coli* (*58*). In bacterial periplasmic transport systems such as the maltose transporter, the substrate-binding protein, the membrane-associated regions, and the ATP binding subunits are synthesized as separate polypeptides and assembled into a functional transporter at the plasma membrane. A conserved sequence motif known as the EAA region (*59*, *60*), mapping within the last intracellular loop of the membrane subunits, is essential for complex assembly and, ultimately, transport (*58*). Mutations in this motif affect transport by preventing association of the peripheral NBDs to the membrane-bound complex (*58*). A mutation (M187I) at the position homologous to T578 in NBD1 was isolated as a second-site suppressor capable of reverting the deleterious effect of EAA motif mutation, restoring the ability to recruit the peripheral NBDs and to carry out maltose transport (*58*). These results, together with those reported here for T578, independently point at T578/M187 as a key position for interaction between the membrane-associated region and the NBDs. They suggest that the mechanism underlying this type of interaction has been preserved through the evolution of the ABC transporter family. Although the EAA region has not been precisely conserved in the evolution of mammalian ABC transporters, one can nevertheless find a remnant of this sequence at the homologous position within the intracellular loop 2 of P-gp (*61*). The possibility that this residue and loop may directly interact with T578 in the NBD1 is currently being tested.

ACKNOWLEDGMENT

We are indebted to Ms. Martine Brault for expert technical assistance.

REFERENCES

1. Gros, P., and Hanna, M. (1996) in *Handbook of Biological Physics 2* (Konings, W. N., Kaback, H. R., and Lolkema, J. S., Eds.) pp 137−163, Elsevier, Amsterdam.
2. Safa, A. R. (1992) *Cancer Invest. 10*, 295−305.
3. Schurr, E., Raymond, M., Bell, J. C., and Gros, P. (1989) *Cancer Res. 49*, 2729- 2734.
4. Hamada, H., and Tsuruo, T. (1988) *J. Biol. Chem. 263*, 1454−1458.
5. Ambudkar, S. V., Lelong, I. H., Zhang, J., Cardarelli, C. O., Gottesman, M. M., and Pastan, I. (1992) *Proc. Natl. Acad. Sci. U.S.A. 89*, 8472−8476.
6. Doige, C. A., Yu, X., and Sharom, F. J. (1992) *Biochim. Biophys. Acta 1109*, 149−160.
7. Al-Shawi, M. K., and Senior, A. E. (1993) *J. Biol. Chem. 268*, 4197−4206.
8. Ruetz, S., and Gros, P. (1994) *J. Biol. Chem. 269*, 12277−12284.
9. Smit, J. J. M., Schinkel, A. H., Oude Elferink, R. P. J., Groen, A. K., Wagenaar, E., van Deemter, L., Mol, C. A. A. M., Ottenhoff, R., van der Lugt, N. M. T., van Roon, M. A., van der Valk, M. A., Offerhaus, G. J. A., Berns, A. J. M., and Borst, P. (1993) *Cell 75*, 451−462.
10. Smith, A. J., Timmermans-Hereijgers, J. L. P. M., Roelofsen, B., Wirtz, K. W. A., van Blitterswijk, W. J., Smit, J. J. M., Schinkel, A. H., and Borst, P. (1994) *FEBS Lett. 354*, 263−266.
11. Ruetz, S., and Gros, P. (1994) *Cell 77*, 1071−1081.
12. van Helvoort, A., Smith, A. J., Sprong, H., Fritzsche, I., Schinkel, A. H., Borst, P., and van Meer, G. (1996) *Cell 87*, 507−517.
13. Gros, P., Croop, J., and Housman, D. (1986) *Cell 47*, 371−380.
14. Ames, G. F.-L., Mimura, C. S., Holbrook, S. R., and Shyamala, V. (1992) *Adv. Enzymol. Relat. Areas Mol. Biol. 65*, 1−47.

15. Kast, C., Canfield, V., Levenson, R., and Gros, P. (1995) *Biochemistry 34*, 4402−4411.
16. Kast, C., Canfield, V., Levenson, R., and Gros, P. (1996) *J. Biol. Chem. 271*, 9240−9248.
17. Loo, T. W., and Clarke, D. M. (1995) *J. Biol. Chem. 270*, 843−848.
18. Raviv, Y., Pollard, H. B., Brugggeman, E. P., Pastan, I., and Gottesman, M. M. (1990) *J. Biol. Chem. 265*, 3975−3980.
19. Greenberger, L. M. (1993) *J. Biol. Chem. 268*, 11417−11425.
20. Devine, S. E., Ling, V., and Melera, P. W. (1992) *Proc. Natl. Acad. Sci. U.S.A. 89*, 4564−4568.
21. Loo, T. W., and Clarke, D. M. (1993) *J. Biol. Chem. 268*, 19965−19972.
22. Loo, T. W., and Clarke, D. M. (1993) *J. Biol. Chem. 268*, 3143−3149.
23. Safa, A. R., Stern, R. K., Choi, K., Agresti, M., Tamai, I., Mehta, N. D., and Roninson, I. B. (1990) *Proc. Natl. Acad. Sci. U.S.A. 87*, 7225−7229.
24. Loo, T. W., and Clarke, D. M. (1994) *J. Biol. Chem. 269*, 7243−7248.
25. Armandola, E. A., Momburg, F., Nijenhuis, M., Bulbuc, N., Fruh, K., and Hammerling, G. J. (1996) *Eur. J. Immunol. 26*, 1748−1755.
26. Anderson, M. P., Gregory, R. J., Thompson, S., Souza, D. W., Paul, S., Mulligan, R. C., Smith, A. E., and Welsh, M. J. (1991) *Science 253*, 202−205.
27. Walker, J. E., Saraste, M., Runswick, M. J., and Gay, N. J. (1982) *EMBO J. 1*, 945- 951.
28. Senior, A. E., Al-Shawi, M. K., and Urbatsch, I. L. (1995) *J. Bioenerg. Biomembr. 27*, 31−36.
29. Scarborough, G. A. (1995) *J. Bioenerg. Biomembr. 27*, 37−41.
30. Azzaria, M., Schurr, E., and Gros, P. (1989) *Mol. Cell. Biol. 9*, 5289−5297.
31. Urbatsch, I. L., Sankaran, B., Bhagat, S., and Senior, A. E. (1995) *J. Biol. Chem. 270*, 26956−26961.
32. Loo, T. W., and Clarke, D. M. (1995) *J. Biol. Chem. 270*, 22957−22961.
33. Beaudet, L., and Gros, P. (1995) *J. Biol. Chem. 270*, 17159−17170.
34. Devault, A., and Gros, P. (1990) *Mol. Cell. Biol. 10*, 1652−1663.
35. Ito, H., Fokuda, K., Murata, K., and Kimura, A. (1983) *J. Bacteriol. 153*, 163−168.
36. Perlin, D. S., Harris, S. L., Seto-Young, D., and Haber, J. E. (1989) *J. Biol. Chem. 264*, 21857−21864.
37. Smith, P. K., Krohn, R. I., Hermanson, G. T., Mallia, A. K., Gartner, F. H., Provenzano, M. D., Fujimoto, E. K., Goeke, N. M., Olson, B. J., and Klenk, D. C. (1985) *Anal. Biochem. 150*, 76−85.
38. Laemmli, U. K. (1970) *Nature 227*, 680−685.
39. Raymond, M., Ruetz, S., Thomas, D. Y., and Gros, P. (1994) *Mol. Cell. Biol. 14*, 277−286.
40. Seto-Young, D., Monk, B. C., and Perlin, D. S. (1992) *Biochim. Biophys. Acta 1102*, 213-219.
41. van Veldhoven, P. P., and Mannaerts, G. P. (1987) *Anal. Biochem. 161*, 45−58.
42. Greenberger, L. M., Yang, C. P., Gindin, E., and Horwitz, S. B. (1990) *J. Biol. Chem. 265*, 4394−4401.
43. Serrano, R. (1991) in *The molecular and cellular biology of the yeast Saccharomyces: genome dynamics, protein synthesis, and energetics 1* (Broach, J. R., Pringle, J. R., and Jones, E. W., Eds.) pp 523−585, Cold Spring Harbor Laboratory Press, Cold Spring Harbor, NY.
44. Hanna, M., Brault, M., Kwan, T., Kast, C., and Gros, P. (1996) *Biochemistry 35*, 3625−3635.
45. Hoof, T., Demmer, A., Hadam, M. R., Riordan, J. R., and Tümmler, B. (1994) *J. Biol. Chem. 269*, 20575−20583.
46. Bakos, E., Klein, I., Welker, E., Szabo, K., Muller, M., Sarkadi, B., and Varadi, A. (1997) *Biochem. J. 323*, 777−783.
47. Loo, T. W., and Clarke, D. M. (1995) *J. Biol. Chem. 270*, 21449−21452.
48. Ruetz, S., Raymond, M., and Gros, P. (1993) *Proc. Natl. Acad. Sci. U.S.A. 90*, 11588−11592.
49. Urbatsch, I. L., Al-Shawi, M. K., and Senior, A. E. (1994) *Biochemistry 33*, 7069−7076.
50. Sharom, F. J., Yu, X., Chu, J. W. K., and Doige, C. A. (1995) *Biochem. J. 308*, 381−390.
51. Sarkadi, B., Price, E. M., Boucher, R. C., Germann, U. A., and Scarborough, G. A. (1992) *J. Biol. Chem. 267*, 4854−4858.
52. Safa, A. R., Agresti, M., Tamai, I., Mehta, N. D., and Vahabi, S. (1990) *Biochem. Biophys. Res. Commun. 166*, 259−266.
53. Kajiji, S., Talbot, F., Grizzuti, K., Van Dyke-Phillips, V., Agresti, M., Safa, A. R., and Gros, P. (1993) *Biochemistry 32*, 4185−4194.
54. Shapiro, A. B., and Ling, V. (1995) *J. Bioenerg. Biomembr. 27*, 7−13.
55. Choi, K., Chen, C.-J., Kriegler, M., and Roninson, I. B. (1988) *Cell 53*, 519−529.
56. Rao, U. S. (1995) *J. Biol. Chem. 270*, 6686−6690.
57. Müller, M., Bakos, E., Welker, E., Váradi, A., Germann, U. A., Gottesman, M. M., Morse, B. S., Roninson, I. B., and Sarkadi, B. (1996) *J. Biol. Chem. 271*, 1877−1883.
58. Mourez, M., Hofnung, N., and Dassa, E. (1997) *EMBO J. 16*, 3066−3077.
59. Dassa, E., and Hofnung, M. (1985) *EMBO J. 4*, 2287−2293.
60. Saurin, W., Koster, W., and Dassa, E. (1994) *Mol. Microbiol. 12*, 993−1004.
61. Shani, N., Sapag, A., and Valle, D. (1996) *J. Biol. Chem. 271*, 8725−8730.
62. Beaudet, L., Urbatsch, I. L. and Gros, P. (1998) *Methods Enzymol.* (in press).

BI972656J